



Bearing capacity of shallow foundations on simulated lunar soil  
by Danmei Gui

A thesis submitted in partial fulfillment of the requirements for the degree of Master of Science in Civil Engineering

Montana State University

© Copyright by Danmei Gui (1995)

Abstract:

Construction of an outpost on the lunar surface requires a thorough investigation of lunar regolith bearing capacity. A series of centrifuge bearing capacity experiments and conventional triaxial compression experiments were performed using a lunar soil simulant, MLS-1, in order to examine the appropriateness of using conventional bearing capacity solutions on lunar regolith.

The preliminary testing programs were designed and conducted to assess the plane strain conditions and the effects of the container walls and bottom on test results. A reasonable minimum depth of soil was determined which prevented effects from the container bottom and a rational configuration of the test footings designed to ensure a plane strain condition was obtained by assessment of the test results. In addition, the bearing capacity values of surface footings and embedded footings on MLS-1 were tested.

In order to obtain accurate bearing capacity predictions, evaluation of shear strength parameters is important. Two different analytical approaches, nonlinear tangent analysis and nonlinear secant analysis, were used to obtain the shear strength parameters of MLS-1. These approaches require the determination of mean normal stress level in the soil. A proposed expression for evaluation of the mean normal stress as a function of friction angle is presented. The shear strength parameters of MLS-1 corresponding to Meyerhofs, Vesic's, and Chen's methods are obtained using this expression. The bearing capacity of MLS-1 was predicted by the aforementioned methods. The bearing capacity values from the experiments and these analytical approaches are compared.

The analysis shows that, for the particular soil property of MLS-1, directly using the conventional approaches to evaluate ultimate bearing capacity cannot give a satisfactory explanation of the experimental results, especially for the problems with embedded footings.

BEARING CAPACITY OF SHALLOW FOUNDATIONS ON  
SIMULATED LUNAR SOIL

BY

DANMEI GUI

A thesis submitted in partial fulfillment  
of the requirements for the degree

of

Master of Science

in

Civil Engineering

MONTANA STATE UNIVERSITY  
Bozeman, Montana

March 1995

N378

G94

**APPROVAL**

of a thesis submitted by

DANMEI GUI

This thesis has been read by each member of the thesis committee and has been found to be satisfactory regarding content, English usage, format, citations, bibliographic style, and consistency, and is ready for submission to the College of Graduate Studies.

15 March, 1995

Date

Lu W. Feli

Chairperson, Graduate Committee

Approved for the Major Department

15 March 1995

Date

Heather E. Long

Head, Major Department

Approved for the College of Graduate Studies

4/26/95

Date

R. Brown

Graduate Dean

## STATEMENT OF PERMISSION TO USE

In presenting this thesis in partial fulfillment of the requirements for a master's degree at Montana State University, I agree that the Library shall make it available to borrowers under rules of the Library.

If I have indicated my intention to copyright this thesis by including a copyright notice page, copying is allowable for scholarly purposes, consistent with "fair use" as prescribed in the U.S. Copyright law. Requests for permission for extended quotation from or reproduction of this thesis in whole or in parts may be granted only by the copyright holder.

Signature Danmei Gu

Date March 27, 1995

## ACKNOWLEDGEMENTS

The author gratefully acknowledges the financial support provided by the NSF EPSCoR MONTS program, by NASA EPSCoR through the Montana Space Grant Consortium Program, and the Engineering Experiment Station at Montana State University.

The author expresses appreciation to Dr. Steven W. Perkins for his guidance and support leading to the completion of this thesis. The author also extends her appreciation to the professors of the Department of Civil Engineering for their guidance in the academic progress of this student.

The author would like to express her appreciation to Dr. Hon - Yim Ko and Dr. Stein Sture of the University of Colorado, Boulder for their advice during the experimental portion of this research. Gratitude is also extended to the staff and the graduate students at the University of Colorado, Boulder for their kind help during the experimental program.

## TABLE OF CONTENTS

	Page
1. INTRODUCTION .....	1
Background and Problem .....	1
Scope of Work .....	6
2. LITERATURE REVIEW .....	10
Introduction .....	10
Principles of Soil - Structure Interaction Modeling .....	11
Principles of Modeling-Similarity .....	12
Conventional Small-Scale Model Tests .....	18
Centrifuge Model Tests .....	18
Experimental Approaches to the Bearing Capacity Problem .....	19
Full-Scale Model Tests .....	20
Small-Scale Model Tests .....	22
Centrifuge Small-Scale Model Tests .....	25
Issues Impacting Centrifuge Model Tests .....	27
Analytical Approaches to the Bearing Capacity Problem .....	31
The Limit Equilibrium Method .....	33
The Slip-Line Method .....	46
The Method of Limit Analysis (Limit Plasticity) .....	50
3. EXPERIMENTAL WORK .....	60
Introduction .....	60
The 400g-ton Centrifuge Facility at the University of Colorado .....	61
Philosophy of Testing Program .....	63
Material Properties .....	65
Experimental Set-up .....	70
Apparatus .....	70
Sample Preparation .....	75
Testing Procedure .....	75
Sample Observation .....	79
Results .....	81
Assessment of The Influence of The Container Walls .....	81
The Assessment of Plane Strain Condition .....	84
Testing Program and Bearing Capacity Results .....	86

## TABLE OF CONTENTS (Continued)

	Page
4. BEARING CAPACITY OF MLS-1 .....	90
Introduction .....	90
The Determination of Shear Strength Parameters for MLS-1 .....	91
The Influence of Stress Level on Shearing Strength Parameter ( $c, \phi$ ) .....	91
The Procedure to Obtain Linear Shear Strength Parameters .....	95
Shear strength parameters ( $c, \phi$ ) of MLS-1 .....	95
Investigation of the Mean Normal Stress $p$ .....	98
Introduction .....	98
Definition of A Dimensionless Factor $B_0$ .....	101
Function of Determining the Mean Normal Stress $p$ .....	103
Bearing Capacity Analysis of MLS-1 .....	107
Bearing Capacity for Surface Footings .....	107
Bearing Capacity For Embedded Footings .....	114
The Slip-line Method for Ultimate Bearing Capacity Analysis .....	116
5. SUMMARY, CONCLUSIONS AND RECOMMENDATIONS FOR FURTHER WORK .....	132
Summary .....	132
Conclusions .....	134
Recommendations For Further Study .....	136
REFERENCES .....	139
APPENDICES .....	144
Appendix A Conventional Triaxial Compression Results .....	145
Appendix B Bearing Capacity Results .....	154
Appendix C Deviation of the Slip-line Method .....	168
Introduction .....	169
Orientation of Slip Lines and Their Relations Conditions of Strain .....	169
Stress Equilibrium Equations .....	170
Solution Via Method of Characteristics .....	172
Numerical Integration .....	174
The Slip-line Solution on Ultimate Bearing Capacity of Shallow Strip Footing .....	178
Appendix D Programs of the Slip-line Method .....	182
Program of Bearing Capacity Computation for Smooth Footing Base .....	183
Program of Bearing Capacity Computation for Partial Rough Footing Base .....	190

## LIST OF TABLES

Table	Page
1. Similarity requirements .....	17
2. Similarity requirements for conventional model and centrifuge model .....	17
3. Bearing capacity equations by several researchers .....	43
4. Shape, depth, and inclination factors for Meyerhof's bearing capacity equation ..	44
5. Shape, depth, inclined and other factors for Hansen and Vesic equations .....	45
6. Comparison of the experimental values of failure surface size in MLS-1 with theoretical values .....	80
7. Experiments performed for the evaluation of influence of container bottom .....	88
8. Experiments performed for the assessment of plane strain condition .....	88
9. Experiments performed for the study of bearing capacity on surface and embedded footing .....	89
10. Shear strength parameters of MLS-1 from CTC peak strength results .....	97
11. Comparison of theoretical and experimental bearing capacity of surface strip footings from peak strength of CTC tests .....	111
12. Comparison of theoretical and experimental bearing capacity of surface strip footings from residual strength of CTC tests .....	111
13. Comparison of theoretical and experimental bearing capacity of embedded strip footings from peak strength of CTC tests .....	117
14. Comparison of theoretical and experimental bearing capacity of embedded strip footing from residual strength of CTC tests .....	118

## LIST OF FIGURES

Figure	Page
1. Forces on (a) the solid phase (b) the liquid phase of a small element of soil . . . . .	12
2. Similarity of stress -strain curves for model and prototype (Rocha,1957) . . . . .	14
3. Relationship between $N_{\gamma q}$ and $\gamma B_n/E_q$ for Toyoura sand (Yamaguchi, 1977) . . . . .	29
4. The effect of self-weight on bearing capacity in centrifugal model . . . . .	30
5. The direction of the resultant force. . . . .	30
6. Mohr's circle and plastic equilibrium . . . . .	34
7. Prandtl failure mechanism (Jumikis, 1984) . . . . .	36
8. Terzaghi's failure mechanism (Terzaghi, 1943) . . . . .	39
9. Different shear failure curve . . . . .	39
10. Meyerhof's failure mechanism (Meyerhof, 1951) . . . . .	41
11. Stress characteristics of drain loading . . . . .	47
12. Bearing capacity calculation based on Hill mechanism . . . . .	55
13. Bearing capacity calculation based on Prandtl mechanism . . . . .	55
14. The 400g-ton centrifuge at University of Colorado, Boulder. . . . .	61
15. Schematics of the 400g - ton centrifuge (Ko, 1990) . . . . .	62
16. The grain size distribution for MLS-1 . . . . .	67
17. The p-q stress space of MLS-1 . . . . .	68
18. The stress-strain curve of a CTC test for confining pressure $\sigma_3 = 650$ kPa . . . . .	69
19. Configuration of footing segments (unit: mm) . . . . .	72

## LIST OF FIGURES (Continued)

Figure	page
20. Configuration of the sample container (unit: mm) .....	73
21. Configuration of the loading system .....	74
22. Sample preparation .....	76
23. Photograph of the blocks .....	77
24. Photograph of the loading system .....	77
25. The evaluation of effect of the container boundary .....	83
26. The evaluation of plane strain condition .....	85
27. Centrifuge bearing capacity results .....	87
28. Mohr's circle and the failure envelope .....	92
29. Shear strength in a p-q plane .....	93
30. Net of Characteristics. ....	100
31. The ranges of the parameters $c/(\gamma B)$ .....	102
32. The relationship between the ratio $(p/q_{ult})$ and the friction angle $\phi$ and non-dimensional factor $B_0$ .....	104
33. The relationship between the ratio $(p/q_{ult})$ and friction angle $\phi$ .....	105
34. Comparison of theoretical and experimental bearing capacity values for surface footing by using the peak tangent shear strength .....	112
35. Comparison of theoretical and experimental bearing capacity values for for surface footings by using the peak secant shear strength .....	113

## LIST OF FIGURES (Continued)

Figure	page
36. Comparison of theoretical and experimental bearing capacity values for embedded footings by using the peak tangent shear strength (25g) .....	119
37. Comparison of theoretical and experimental bearing capacity values for embedded footings by using the peak tangent shear strength (16.7g).....	120
38. Comparison of theoretical and experimental bearing capacity values for embedded footings by using the peak tangent shear strength (5g) .....	121
39. Comparison of theoretical and experimental bearing capacity values for embedded footings by using the peak secant shear strength (25g) .....	122
40. Comparison of theoretical and experimental bearing capacity values for embedded footings by using the peak secant shear strength (16.7g).....	123
41. Comparison of theoretical and experimental bearing capacity values for embedded footings by using the peak secant shear strength (5g) .....	124
42. The percentage difference of the theoretical and experimental bearing capacity for surface footing.....	125
43. The percentage difference of the theoretical and experimental bearing capacity for embedded footings (25g).....	126
44. The percentage difference of the theoretical and experimental bearing capacity for embedded footings (16.7g) .....	127
45. The percentage difference of the theoretical and experimental bearing	

## LIST OF FIGURES (Continued)

Figure	page
capacity for embedded footings (5g) .....	128
46. Chart for mean non- dimensional pressure with non - dimensional width for smooth footing base.....	130
47. Chart for mean non - dimensional pressure with non - dimensional width for partial rough footing base .....	131
48. The relationship between the ratio ( $p/q_{ult}$ ) and friction angle obtained from experimental results and from new definition of mean normal stress.....	138
49. CTC experiment on MLS-1 at $\sigma_3 = 750 \text{ kPa}$ .....	146
50. CTC experiment on MLS-1 at $\sigma_3 = 650 \text{ kPa}$ .....	146
51. CTC experiment on MLS-1 at $\sigma_3 = 650 \text{ kPa}$ .....	147
52. CTC experiment on MLS-1 at $\sigma_3 = 500 \text{ kPa}$ .....	147
53. CTC experiment on MLS-1 at $\sigma_3 = 500 \text{ kPa}$ .....	148
54. CTC experiment on MLS-1 at $\sigma_3 = 350 \text{ kPa}$ .....	148
55. CTC experiment on MLS-1 at $\sigma_3 = 200 \text{ kPa}$ .....	149
56. CTC experiment on MLS-1 at $\sigma_3 = 200 \text{ kPa}$ .....	149
57. CTC experiment on MLS-1 at $\sigma_3 = 150 \text{ kPa}$ .....	150
58. CTC experiment on MLS-1 at $\sigma_3 = 150 \text{ kPa}$ .....	150
59. CTC experiment on MLS-1 at $\sigma_3 = 100 \text{ kPa}$ .....	151
60. CTC experiment on MLS-1 at $\sigma_3 = 100 \text{ kPa}$ .....	151

## LIST OF FIGURES (Continued)

Figure	page
61. CTC experiment on MLS-1 at $\sigma_3 = 50 \text{ kPa}$ .....	152
62. CTC experiment on MLS-1 at $\sigma_3 = 50 \text{ kPa}$ .....	152
63. CTC experiment on MLS-1 at $\sigma_3 = 50 \text{ kPa}$ .....	153
64. Bearing capacity result of BC3a01.O <sub>1</sub> .....	155
65. Bearing capacity result of BC3d01.O <sub>2</sub> .....	155
66. Bearing capacity result of BC3d01.O <sub>3</sub> .....	156
67. Bearing capacity result of BC3a01.O <sub>4</sub> .....	156
68. Bearing capacity result of BC3c01.O <sub>5</sub> .....	157
69. Bearing capacity result of BC1a01.O <sub>6</sub> .....	157
70. Bearing capacity result of BC1c01.O <sub>7</sub> .....	158
71. Bearing capacity result of BC3b01.O <sub>8</sub> .....	158
72. Bearing capacity result of BC3a01.O <sub>9</sub> .....	159
73. Bearing capacity result of BC3a01.O <sub>10</sub> .....	159
74. Bearing capacity result of BC3c01.O <sub>11</sub> .....	160
75. Bearing capacity result of BC2b01.O <sub>12</sub> .....	160
76. Bearing capacity result of BC1b01.O <sub>13</sub> .....	161
77. Bearing capacity result of BC2b02.O <sub>14</sub> .....	161
78. Bearing capacity result of BC2b12.O <sub>15</sub> .....	162
79. Bearing capacity result of BC2b11.O <sub>16</sub> .....	162

## LIST OF FIGURES (Continued)

Figure	page
80. Bearing capacity result of BC2b22.O <sub>17</sub> .....	163
81. Bearing capacity result of BC2b03.O <sub>18</sub> .....	163
82. Bearing capacity result of BC2b21.O <sub>19</sub> .....	164
83. Bearing capacity result of BC2b13.O <sub>20</sub> .....	164
84. Bearing capacity result of BC2b23.O <sub>21</sub> .....	165
85. Bearing capacity result of BC2b21.O <sub>22</sub> .....	165
86. Bearing capacity result of BC2b21.O <sub>23</sub> .....	166
87. Bearing capacity result of BC9c01.O <sub>24</sub> .....	166
88. Bearing capacity result of BC3b01.O <sub>25</sub> .....	167
89. Orientation of the stress plane .....	169
90. Mohr-Coulomb circle .....	170
91. Pandtl singularity for Goursat solution .....	179
92. Direction of major principal stress for different roughness of footing bases .....	181

**ABSTRACT**

Construction of an outpost on the lunar surface requires a thorough investigation of lunar regolith bearing capacity. A series of centrifuge bearing capacity experiments and conventional triaxial compression experiments were performed using a lunar soil simulant, MLS-1, in order to examine the appropriateness of using conventional bearing capacity solutions on lunar regolith.

The preliminary testing programs were designed and conducted to assess the plane strain conditions and the effects of the container walls and bottom on test results. A reasonable minimum depth of soil was determined which prevented effects from the container bottom and a rational configuration of the test footings designed to ensure a plane strain condition was obtained by assessment of the test results. In addition, the bearing capacity values of surface footings and embedded footings on MLS-1 were tested.

In order to obtain accurate bearing capacity predictions, evaluation of shear strength parameters is important. Two different analytical approaches, nonlinear tangent analysis and nonlinear secant analysis, were used to obtain the shear strength parameters of MLS-1. These approaches require the determination of mean normal stress level in the soil. A proposed expression for evaluation of the mean normal stress as a function of friction angle is presented. The shear strength parameters of MLS-1 corresponding to Meyerhof's, Vesic's, and Chen's methods are obtained using this expression. The bearing capacity of MLS-1 was predicted by the aforementioned methods. The bearing capacity values from the experiments and these analytical approaches are compared.

The analysis shows that, for the particular soil property of MLS-1, directly using the conventional approaches to evaluate ultimate bearing capacity cannot give a satisfactory explanation of the experimental results, especially for the problems with embedded footings.

## CHAPTER ONE

### INTRODUCTION

#### Background and Problem

Among the proposals for future U.S. space program missions, one is returning to the moon to establish a permanent outpost. This moon base would include radio and optical telescopes which, along with other base facilities, must be placed on the lunar soil. The construction of lunar bases will be conceptually similar in many ways to the construction of terrestrial facilities. Extraterrestrial engineering requires, however, different approaches both in terms of technology and in philosophy. The major philosophical difference will be the approach to the "exactness" of our designs. It may be said that commonplace terrestrial civil structures are relatively inexact, in that large factors of safety are incorporated to insure successful operation, resulting in excessive use of materials and workmanship. Lunar facilities will require the incorporation of load and resistance factors that are clearly defined and do not result in excessive factors of safety. This in turn requires an accurate understanding of the mechanics of these structures and their interaction with the lunar environment. Hence, the extraterrestrial engineer must employ new

technological tools in such a way that an accurate picture of the functional ability of constructed lunar facilities emerges prior to construction itself.

Basic geotechnical engineering properties of lunar regolith became available through the Apollo lunar landings. The lunar regolith has been defined as a stratum of debris of relatively low cohesion that overlies a more coherent substratum. The composite regolith mass is described as a fine silty sand with nearly 40% characterized as silt with particle size smaller than 100 micrometers. Various estimates have been made of the cohesion and the friction angle of the regolith. These estimates have relied on the observation and analysis of the interaction of loaded surfaces with the native regolith. It was found that the cohesion ranges from nearly zero to 4 *kPa* with the friction angle ranging from approximately 40° to 60°. The low values of friction angle and cohesion pertain to loose regolith (regolith with low relative density) and the high values to very dense regolith (regolith with a high relative density). Dry terrestrial sands commonly do not possess any cohesion. Even though the cohesion is relatively small, it plays an important role in the engineering solution of many soil mechanics problems.

Since working with real lunar regolith is difficult from the standpoint of availability, a simulant has been developed which matches the more significant engineering properties of lunar regolith. This soil is known as Minnesota Lunar Simulant (MLS-1) and is described by Weiblen and Gordon (1989). Perkins (1991) has performed an extensive series of laboratory strength and deformation experiments to characterize the stress-strain properties of MLS-1. In general, it was found that the frictional characteristics of real lunar regolith could be closely matched. It was difficult to match the cohesion levels

observed for lunar regolith. This was due, in part, to the absence of aggregated particles and the absence of electrostatic attractive forces between soil particles.

The construction of structures on the lunar surface, like the construction of terrestrial structures, requires a thorough investigation of stability behavior of the lunar soil such as its bearing capacity. Conventional analysis of stability problems in soil mechanics relies typically upon the soil's frictional and cohesive strength parameters. Bearing capacity solutions, used to establish the ultimate load carrying capacity of shallow foundations, are expressed in terms of bearing capacity factors which are expressed as analytical functions of the friction angle. These solutions have been verified only for soil of relatively modest friction angles (less than  $50^\circ$ ). These bearing capacity factors, and the resulting ultimate bearing capacity of the foundation, are quite sensitive to small changes in the friction angle for friction angles exceeding  $50^\circ$ .

Friction angles for lunar regolith and MLS-1 range from  $41^\circ$  to  $60^\circ$  (Perkins, 1991). Most bearing capacity factor charts stop at  $\phi = 40^\circ$  and never go beyond  $\phi = 50^\circ$ , however. Since the assumed modes of failure for soils with very high friction angles have not been investigated, it is difficult to comment on the appropriateness of the formulation of the bearing capacity, particularly the term  $N_\gamma$ . Perkins (1991) conducted finite element analyses of a surface footing bearing on dense MLS-1. The material model was calibrated from conventional laboratory strength versus deformation experiments using dense MLS-1, where the peak friction angle was as great as  $60^\circ$ . It was found that conventional bearing capacity theory overpredicted the peak bearing pressure as compared to that

determined from the finite element analyses. The results indicated the need for further study and analysis of bearing capacity theory in general, before applying this theory to the design and construction of lunar base facilities.

Experimental model tests have a very significant meaning in the evaluation of existing theories used for bearing capacity problems. Three different types of model tests, full-scale model tests, small-scale model tests under 1-g environment and centrifuge small-scale model tests, have been performed by various researchers on different soils. Experimental difficulties and expense tend to prohibit full scale testing and only a few full scale tests have been reported in the literature in the last few decades. Small-scale 1-g model tests do not satisfy most similitude requirements for dimensional analysis, and these small-scale tests are believed to result in a significant discrepancy between the experimental results and extrapolated field behavior.

An importance in determining the bearing capacity of strip footings is the assumption of plane strain inherent in most theoretical approaches. When performing footing tests, the maintenance, as closely as possible, of plane strain conditions is important so that the experiments will be carried out under the same conditions as assumed in the theories. Many researchers have tried to create a condition of plane strain in different ways.

To the author's knowledge, one disadvantage, in many previous bearing capacity experiments, is that sample containers were too small to allow the entire failure plane to develop. The rigidity of containers certainly influences test results. The basic theoretical assumption of a complete failure plane in failed soil could be violated due to the above

problems.

An accurate prediction of the bearing capacity of a soil largely depends on the analysis method used for the shear strength obtained from conventional triaxial tests. In most cases, a linear Mohr-Coulomb strength criterion is widely used to describe shear strength. For many soils, a linear Mohr-Coulomb strength criterion is an approximation of the actual non-linear shape of the failure envelope. This curvature should be taken into account if more realistic bearing capacity solutions are to be expected. As a consequence, the friction angle,  $\phi$ , depends upon normal stress in a material of a given density. Conventional bearing capacity solutions, however, rely upon the use of constant friction angle and cohesion. Since the results obtained by conventional triaxial compression tests for MLS-1 provided a nonlinear relation between the shear strength parameters and normal stress, normal stress then has to be determined first in order to obtain some estimate of a linear friction angle and cohesion.

In determining a soil's normal stress state the physical characteristics of the footing must be considered in addition to the soil's mechanical properties. Various assumptions have been made by researchers in order to simplify the determination of the normal stress state. Meyerhof (1948) suggested taking the mean normal stress to be one tenth the applied average ultimate bearing capacity for friction angles in the range of  $45^\circ$  to  $46^\circ$ . This is thought, however, to be limited and arbitrary.

### Scope of Work

The objective of this thesis is to examine existing and improved methods for the design of foundations and for the analysis of bearing capacity using simulated lunar regolith, MLS-1, compacted in a very dense state and possessing very high friction angles. Load versus displacement experiments were performed on models of footings tested in an elevated gravity fields. The results are compared to predictions using conventional analysis methods, a numerical analysis method and the limit plasticity method.

The previous section introduced the background of the research and defined the problems to be addressed in this thesis. The tasks that need to be accomplished to solve the various issues were outlined in general terms. This section defines how the solution can be reached in more specific terms and provides a description of the contents of the remaining Chapters to this thesis.

As indicated in the previous section, full-scale model tests are usually impractical due to expense, while 1-g small-scale model tests cannot achieve adequate similarity requirements because of reduced dimensions. In order to satisfy similitude requirements, centrifuge small-scale model tests were designed to test the bearing capacity of shallow foundations on MLS-1. In general, the similitude requirements state that a model scaled down from prototype dimensions by a factor of  $n$  must be tested in a gravity field whose magnitude is increased from the prototype gravity field by the same factor  $n$ . This is easily accomplished in a geotechnical centrifuge and has been shown to produce valid results for

terrestrial applications. The experimental work undertaken in this thesis has two major advantages over the previous studies: (1) plane strain conditions were examined effectively from a preliminary testing program and plane strain conditions were modeled properly in the bearing capacity experiments. (2) A reasonable preliminary testing program was designed and conducted to evaluate the effects of the container boundary on the test results, so that the effects were prevented from influencing the experimental results.

In order to model plane strain conditions in the centrifuge experiments, the footing feature was designed to provide as well as to evaluate plane strain conditions. The composite footing was constructed of five segments, where the three interior segments each had a length equal to its width  $B$ , and the two end segments could be interchanged with various strip footings of length varying from  $1B$  to  $3B$ . The conditions required to achieve plane strain can be assessed from the experimental results through variation of the footing lengths for the same  $g$ -level and sample.

In order to avoid the influence of the container boundaries, the test program was designed to test different depths of soil under the same  $g$  level and the same footing dimension. By the assessment of these test results, a minimum height of the sample could be obtained to prevent the influence of the container boundaries on test results.

As mentioned in the above section, evaluation of shear strength analysis parameters is very important in order to obtain accurate bearing capacity predictions, especially for high friction soils. In this thesis, two different analytical approaches, nonlinear tangent analysis and nonlinear secant analysis, were used to obtain the shear strength of MLS-1.

Using the tangent analysis method, the friction angle,  $\phi$ , can be obtained by taking the slope of tangent of the failure envelop, and the cohesion,  $c$ , can be obtained by the intersection of the tangent line with the shear stress axis. Using the secant analysis, where the cohesion is assumed to be zero, a straight line can be drawn from the origin to a point on the failure curve and the secant friction angle can be obtained from the slope of the straight line. The curvature of the failure envelop was taken into account in both the analytical methods.

In order to obtain linear values of friction angle and cohesion, a general function for determining an average normal stress state corresponding to soil properties and footing physical conditions was produced. The slip-line method was used to determine ultimate bearing capacity and mean normal stress in a soil, and the ratio of average mean normal stress to ultimate bearing capacity was obtained to be a function of friction angle.

The next chapter of this thesis begins with a succinct presentation of principles of modeling. This section will describe the similarity laws of modeling, and the principles of conventional small-scale model tests, and centrifuge model tests are presented. The content in this section constitutes the theoretical supporting structure for the centrifuge experiment methodology used to study the bearing capacity problems on MLS-1. The previous experimental work related to the bearing capacity problem will be reviewed in this chapter, which includes full-scale model tests, small-scale model tests as well as centrifuge model tests. The theoretical approaches applied to the analysis of bearing capacity problems such as limit analysis, slip-line, and limit plasticity will also be reviewed in light of this thesis. The impacts of centrifuge model tests will be discussed for

a further understanding of centrifuge model tests.

Chapter three presents the experimental work for the bearing capacity research of shallow foundations on MLS-1. This chapter is concerned with the philosophy of the testing program, the techniques of the sample preparation, the experimental procedure, as well as the assessment of plane strain conditions and boundary effects of the container. The properties of MLS-1 used in this study will be described in this chapter where the failure criterion of the material was derived from CTC results. Detailed results of CTC tests and bearing capacity experiments are given in Appendix A and Appendix B, respectively.

Chapter four presents a comparison of analytical results predicted from existing theories and methods such as Meyerhof, Vesic, Chen and the slip-line method with the experimental results. From these predictions, conclusions will be made regarding the suitability of these analysis methods for lunar applications. In order to analyze the experimental results adequately, two analysis approaches ("tangent" and "secant" analyses) to obtain shear strength parameters of the soil will be discussed first, and the shear strengths obtained from these two approaches will be presented in the first section of this chapter. The numerical solution for slip-line method will be presented and the bearing capacity values obtained from this method will be compared with the experimental results as well as aforementioned predictions. The detailed solution of the slip-line method is presented in Appendix C, and the computer program for the slip-line method will be presented in Appendix D.

## CHAPTER TWO

### LITERATURE REVIEW

#### Introduction

The literature review in this chapter consists of three sections: principles of soil-structure interaction modeling, experimental approaches to bearing capacity problems, and analytical approaches to bearing capacity problems. In the first section, the similarity laws of modeling are succinctly discussed, and the principles of conventional small-scale model tests, and centrifuge model tests are presented. The content in this section constitutes the theoretical supporting structure for the centrifuge experiment methodology used to study the bearing capacity problems on the simulated lunar soil (MLS-1). The second section introduces the issues of experimental approaches to bearing capacity problems, which include three approaches of full-scale model tests, small-scale model tests as well as centrifugal small-scale model tests. Several issues impacting centrifuge model tests are discussed in this section. The remaining section is a presentation of issues related to theoretical approaches to the bearing capacity problems, which form the theoretical backbone for the analysis techniques in later chapters. These issues include the

limit equilibrium analytical method, the slip-line method, and the method of limit analysis applied to bearing capacity studies.

### **Principles of Soil - Structure Interaction Modeling**

Soil engineering problems such as stability of slopes, earth pressure, bearing capacity etc., are usually solved by using theories based on a set of simplifying assumptions, which may not be valid in all conditions and may lead to erroneous conclusions. Prior to the construction of an important structure, it is desirable to conduct a large scale field test in order to validate that behavior of the footing matches the predictions if the analytical technique used. The cost, however, and time it requires and the difficulty in controlling the test conditions reduce the value of the field test for research purposes. On the contrary, laboratory reduced scale model tests have two advantages compared with full scale or field experiments: (1) they allow study of the behavior of structures under different conditions; and (2) they are relatively rapid, inexpensive and easy to operate.

The development of models for geotechnical analysis includes the following steps: (1) choice of materials satisfying laws of similitude; (2) construction of the model; and (3) application of the loadings and observation of the model. The following sections will present a discussion of the similarity laws and the principles of conventional small-scale model tests as well as centrifuge model tests.

### Principles of Modeling - Similarity

The rational study of all model tests must be based upon considerations of the requirements for achieving adequate similarity between the field prototype and the model. The equality of stresses between a model and the prototype built of the same materials is crucial to the maintenance of any reasonable similarity in models of particulate assemblies such as soil. In order to demonstrate the principle of similarity, consider a small element of volume  $V$  contained within a larger body of a granular medium (Roscoe, 1968). The entire body is saturated with a pore fluid which is flowing through the skeleton. Considering the volume as two distinct phases (solid and liquid), as shown in Figure 1(a), the local value of the porosity, i.e. ratio of voids to total volume, is  $k$  for the element, and the unit weight of the solid material is  $\gamma_s$ . The forces on the solid phase of the element are (1) the self-weight of the solid  $\gamma_s(1-k)V$  acting vertically downwards, (2) the upward thrust of the fluid displaced by the grain  $\gamma_f(1-k)V$ , where  $\gamma_f$  is the unit weight of the fluid, (3) the net resultant  $\sigma'_{ij}S$  of the effective stresses acting on the boundary surface of

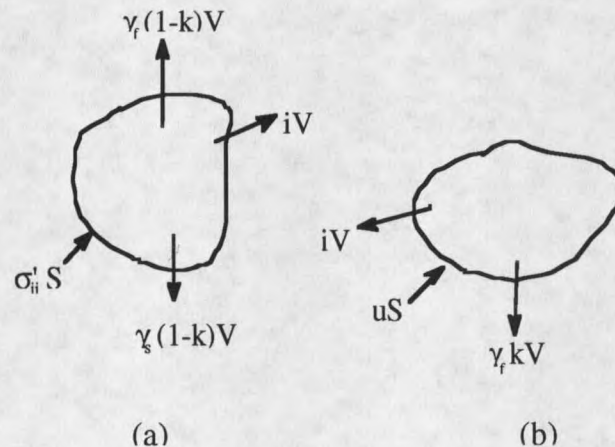


Figure 1. Forces on (a) the solid phase (b) the liquid phase of a small element of soil

the element, and (4) the seepage force  $iV$  due to the hydraulic gradient causing fluid flow through the element, where  $i$  is the seepage force per unit volume

The forces on the fluid phase within the element are shown in Figure 1(b), and are (1) the seepage force  $iV$  in the opposite direction to that in Figure 1(a), (2) the self-weight of the fluid  $\gamma_f kV$  vertically downwards, and (3) the net resultant  $uS$  of the pore-water pressure on the boundary of the element.

Assume that two such elements are homologous in the prototype and in the model, and that the medium used in the prototype has a unique stress-strain curve which is not necessarily linear, but is independent of time. Let the linear length scale ratio between prototype and model be  $h$  (where  $h > 1$ ). There is  $V_p = h^3 V_m$  for the two elements where the subscripts  $p$  and  $m$  refer to prototype and model, respectively. In addition, assume that the medium used in the model has a similar stress-strain curve as the prototype material obeying the same restrictions but in which all stresses are scaled down by the ratio  $1/\alpha$  and all strains by the ratio  $1/\beta$ . This condition is illustrated in Fig.2 (Rocha, 1957). With these assumptions it is now possible to develop the condition of similarity if data from the model are to be used to predict the behavior of the prototype.

For similarity all stresses, including pore-water pressure, must be to the scale and consequently all forces to the scale  $h^2\alpha$ . Scaling the self-weight of the solid phases then requires that:

$$\frac{\gamma_{sp}(1-k_p)V_p}{\gamma_{sm}(1-k_m)V_m} = h^2\alpha \quad (1)$$

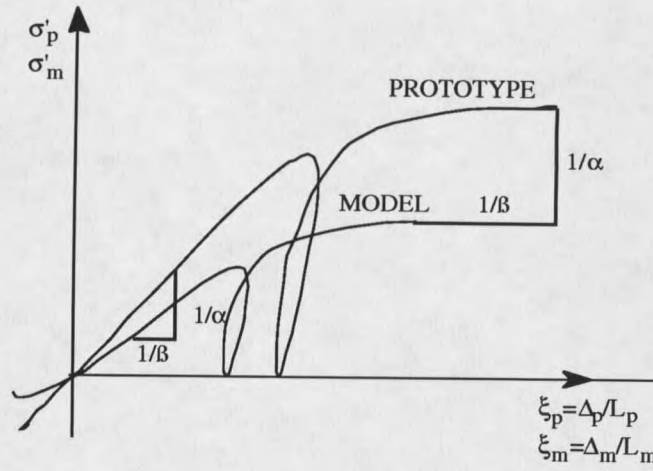


Figure 2. Similarity of stress -strain curves for model and prototype (Rocha,1957)

If  $\gamma_{sp} = n_s \gamma_{sm}$  is used, where  $n_s$  is the scale factor for the unit weights of the solid materials, this requirement in equation (1) becomes:

$$\alpha = hn_s \frac{1 - k_p}{1 - k_m} \quad (2)$$

where the length scale has been applied to the volume terms. Likewise, scaling the uplift force due to the liquid phase  $\gamma_f(1-k)V$  requires that:

$$\alpha = hn_f \frac{1 - k_p}{1 - k_m} \quad (3)$$

and scaling the self-weight of the liquid phase  $\gamma_f k V$  requires that:

$$\alpha = hn_f \frac{k_p}{k_m} \quad (4)$$

From the equations (3) and (4), it is evident that:

$$k_m = k_p \quad (5)$$

Inserting the condition  $k_m = k_p$  in equations (4) and (5) then requires that  $n_s = n_f$ . The bulk unit weight of a saturated medium is given by  $\gamma = k \gamma_f + (1-k) \gamma_s$  and if  $n$ , the scale factor for the bulk unit weight, is defined by  $\gamma_f = n \gamma_m$ , then, provided  $k_m = k_p$  and  $n_s = n_f$ , it follows that

$$n = n_s = n_f \quad (6)$$

If equations (5) and (6) are satisfied, the following equation can be written:

$$\alpha = hn \quad (7)$$

Equations (5), (6) and (7) specify the conditions that the materials must satisfy for similarity to prevail if all effects of migration of the pore water are ignored, provided that the initial assumptions regarding their stress-strain behavior are satisfied. The quantities listed in Table 2.1 should then scale as shown.

For most modeling applications, the length scale will range from 10 to perhaps 100. The minimum value of the unit weight scale for fluids is approximately 0.7. From equation (7) it is then seen that the stress scale must range from 7 to 70 for most applications. This requires the fabrication of a soil which is quite weak, and thereby difficult to handle. To avoid this problem, and any accompanying difficulties with the fabrication of such a soil, it is convenient to use a model soil such as that  $\alpha = 1$ . This then requires that:

$$h = \frac{1}{n} \quad (8)$$

This indicates that it is necessary to increase the soil and fluid unit weight by the reduction in the length scale. The quantities given in table 1 then reduce to:

$$L_p = nL_m; F_p = \frac{F_m}{n^2}; \sigma_p = \sigma_m; \epsilon_p = \epsilon_m; \gamma_p = n\gamma_m; k_p = k_m \quad (9)$$

For bearing capacity problems of shallow foundations, it is usually considered that, under a plane strain condition, nine independent quantities might influence load versus deflection curve for the foundation which are:

- $\gamma$  ( $N/m^3$ )    the unit weight of soil
- $B$  (m)        the width of a footing
- $D$  (m)        the initial embedment of the footing
- $e$              the void ratio of the soil
- $\phi$             the internal friction angle of the soil
- $c$  ( $N/m^2$ )    the cohesion of the soil
- $\sigma_g$  ( $N/m^2$ ) the crushing strength of the grain material
- $E_g$  ( $N/m^2$ )    the coefficient of elasticity of the grain material
- $d_g$  (m)      the average grain size

The quantities entering into the problem contain two basic units, length and force. In dimensional analysis the quantities  $B$  and  $P_p$  are chosen to represent the basic units and the peak load  $P_p$  of the footing can be expressed in dimensionless form as a function of seven independent dimensionless parameters in the following way (Ovesen, 1979):

$$\frac{P_p}{\gamma B} = F\left(e, \phi, \frac{c}{\gamma B}, \frac{\sigma_g}{\gamma B}, \frac{E}{\gamma B}, \frac{d_g}{\gamma B}, \frac{D}{B/n}\right) \quad (10)$$

Table 1 Similarity requirements of modeling:

Quantity	Scale Factor	Relationship
Length	$1/h$	$L_p = L_m/h$
Force	$h^2\alpha$	$F_p = h^2\alpha F_m$
Stress	$1/\alpha$	$\sigma_p = \sigma_m/\alpha$
Strain	$1/\beta$	$\epsilon_p = \epsilon_m/\beta$
Unit Weight ( Fluid, Solid )	$n$	$\gamma_p = n\gamma_m$
Porosity	$1$	$k_p = k_m$

Table 2 Similarity requirements for conventional model and centrifuge model

No.	Prototype	Conventional Model		Centrifuge Model	
	gravity: $g$	gravity: $g$		gravity: $ng$	
1	$e$	$e$	similar	$e$	similar
2	$\phi$	$\phi$	similar	$\phi$	similar
3	$\frac{c}{\gamma B}$	$\frac{c}{(\gamma B/n)}$	not similar	$\frac{c}{(\gamma n B/n)}$	similar
4	$\frac{\sigma_g}{\gamma B}$	$\frac{\sigma_g}{(\gamma B/n)}$	not similar	$\frac{\sigma_g}{(\gamma n B/n)}$	similar
5	$\frac{E_g}{\gamma B}$	$\frac{E_g}{(\gamma B/n)}$	not similar	$\frac{E_g}{(\gamma n B/n)}$	similar
6	$\frac{d_g}{\gamma B}$	$\frac{d_g}{(B/n)}$	not similar	$\frac{d_g}{(B/n)}$	not similar
7	$\frac{D}{B}$	$\frac{D/n}{B/n}$	similar	$\frac{D/n}{B/n}$	similar











































































































































































































































































































































































